

DETECTION OF CRITICAL DENSITIES ASSOCIATED WITH PIÑON–JUNIPER WOODLAND ECOTONES

BRUCE T. MILNE, ALAN R. JOHNSON, TIMOTHY H. KEITT,
COLLEEN A. HATFIELD, JOHN DAVID, AND PETER T. HRABER
Department of Biology, University of New Mexico, Albuquerque, New Mexico 87131 USA

Abstract. The interfaces between piñon–juniper canopies and grasslands in the southwestern USA present an opportunity to use the modern theory of spatial phase transitions as a formal characterization of ecotone structure. The theory requires an estimation of a critical value of tree cover at which the woodlands switch abruptly from a fragmented collection of small patches of trees to a network of connected canopies. Presumably, this transition is associated with critical environmental conditions that regulate the ecologies of trees vs. grasses. We developed and tested a new method to estimate the critical cover value of woodlands on complex terrain. The method was based on multiscale assessments of the associations between local tree coverage and two types of patch edge. Tests on artificial gradient percolation maps revealed an interaction between the type of edge used (“hull edge,” which is based on only the orthogonal connections between canopy-occupied cells, vs. “accessible edge,” which is based on both orthogonal and diagonal connections between canopy-occupied cells) and the neighborhood rule used to define a cluster (von Neumann 5-cell or Moore 9-cell). When applied to digitized, geographically referenced aerial photographs, the method indicated that areas ≤ 6.6 ha exhibited the theoretical critical value of 59.3% cover predicted for square lattices and the 5-cell neighborhood. Construction of both edge types on a given map can reveal locations of steep environmental gradients that may be buffered against modest climate fluctuations. The edges can be used in the calibration of independent variables to predict tree cover. The agreement between the expected and observed critical densities will motivate extensions of phase transition theory to studies of ecotones in real landscapes.

Key words: *accessible edge; critical phenomena; ecotones; fragmentation; gradient percolation; grasslands; hull edge; Juniperus monosperma; percolation; Pinus edulis; spatial phase transitions; woodlands.*

INTRODUCTION

Ecologists have shown interest in diverse phenomena that fit the generalized notion of a phase transition. Theoretical studies of pattern formation and predator–prey interactions identify critical thresholds that govern patch size diversity, species coexistence, and pattern development (Levin and Paine 1974, Murray and Mimura 1978, Murray 1984, Levin and Segel 1985). Yamamura (1976) treats ecotones (Odum 1959, Botkin et al. 1972, Holland et al. 1991) as ecological phase transitions governed by interactions between population growth rates and intra- versus inter-specific competition. Simplifying assumptions enable Yamamura (1976) to relate specific, critical values of demographic parameters to 1-dimensional transects across landscapes and thereby predict where sharp edges form between species distributions. O’Neill et al. (1989) and Kay and Schneider (1992) discuss the dynamics of systems near a transition, or bifurcation, while Gosz and Sharpe (1989) apply bifurcations to ecological transition zones. Following Rosen (1989), who explores an intriguing analogy between ecosystem dynamics and

behaviors exhibited by the van der Waals equation for ideal gases, Milne et al. (1992) use a critical point in time to inter-relate the dynamics of animals that forage at different rates. Thus, phase transition theory is applicable to the study of ecotones (Holland et al. 1991), succession, epidemics, the spread of disturbance, population outbreaks, and the responses of ecosystems to climate change.

Tests of hypotheses about ecotone generation via phase transitions may have been precluded by the difficulty of modelling phase transition manifolds (Ouimet and Legendre 1988), such as those of Thom (1975) and Yamamura (1976), and by the difficulty of demonstrating that a competitive equilibrium has been reached. Despite the development of recent models (Eagleson and Segarra 1985, Peters and Darling 1985, Neilson 1993, Noble 1993), a falsifiable formalism for the structure and dynamics of ecotones is still needed (Fortin 1994) to explicitly accommodate the sensitivity of ecotones to small changes in environmental conditions at multiple scales.

A rich conceptual framework for ecotones is suggested by theory and observation. On one hand, the abrupt domination by one species can be represented by a threshold effect of environmental or biotic factors

¹ Manuscript received 28 October 1994; revised and accepted 5 July 1995; final version received 4 August 1995.

PLATE 1. Density dependence of the accessible edges of artificial and empirical percolation clusters. (A) Gradient percolation map of occupied cells (green) with accessible edge of spanning cluster (red line); probabilities within each column vary from $p = 0$ (left) to $p = 1.0$ (right). (B, C, D) Subsets of occupied cells (red) for which density in the surrounding region equals $0.5928 \pm 5\%$ of cells occupied in windows of length 5, 15, and 50 cells, respectively. Accessible-edge cells that intersected locations at critical density (yellow) were compared to those that did not intersect (white). Magnification of C (inset) shows details. (E) 39.3-ha map of piñon-juniper woodland (green) and grassland (black) with accessible edge of largest cluster (red). (F, G, H) Subsets of tree cells (red) for which density measured with windows of length 12.7, 38.1, and 127 m was within 5% of $p_c = 0.5928$.

→

(Yamamura 1976, Eagleson and Segarra 1985, Arris and Eagleson 1994); these models predict the state of each point without reference to the influences of surrounding points. On the other hand, since both ecotone geometry and species co-occurrences vary regularly with scale (Milne 1991, 1992, Scheuring and Riedi 1994, Risser 1995, Solé and Manrubia 1995) constraints at broad scales may affect dynamics at fine scales such that the geometry of the ecotone influences its ontogeny. One mechanism for such a hierarchy (Allen and Starr 1982) would be a shift in the ratio of intra- to inter-specific competition (Yamamura 1976) as a function of scale. Thus, a multiscale, spatially explicit approach to ecotone studies would extend ecotone models to complex landscapes and connect events that operate at the local level to those of biogeographic interest (see Cody 1989).

We present a formalism for the study of ecotones and provide methods to identify a critical canopy coverage presumably associated with environmental conditions at which vegetation changes abruptly from grassland to woodland. We build upon techniques developed in studies of physical systems and estimate critical tree coverages at which spatial phase transitions (Domb and Lebowitz 1988) may occur at any number of scales. Our approach accommodates both the notion of critical conditions (Yamamura 1976) and the multiscale nature of ecotone structure.

Ecotones as spatial phase transitions

One of the liveliest areas in the physical sciences is the study of condensed matter, particularly the emerging theory of spatial phase transitions, critical phenomena, and scale dependence (Zallen 1983, Domb and Lebowitz 1988). The field has attracted interest because seemingly unrelated physicochemical processes display a great deal of qualitative, and often quantitative, similarity. Phase transition theory is applied both to changes in the state of matter (e.g., the freezing of a liquid into a solid) and to such diverse phenomena as magnetization, polymerization, gelation, laser transitions, mechanical and electrical properties of disordered materials, and the onset of turbulence (Zallen 1983). These systems exhibit fundamental changes in phase, organization, or spatial structure at critical values of controlling factors such as temperature or density. The phase transition perspective has been applied to theoretical studies of fire spread (MacKay and Jan

1984, Ohtsuki and Keyes 1983a) and the spatial propagation of epidemics (Grassberger 1983, Ohtsuki and Keyes 1983b).

Spatial phase transitions imply the propagation of fine-scale, atomistic interactions over long distances. Amplification of atomistic processes by positive feedbacks (DeAngelis et al. 1986), as for example in growth processes (Meakin 1983), is central to our conceptualization of ecotones. A transect across an ecotonal phase transition should reveal that hydraulic (Eagleson and Segarra 1985) and mesoclimatic (Pielke and Avissar 1990) interactions between contrasting canopies, such as grasses and trees, change suddenly at a particular density. For instance, microclimatic controls on nutrient processing rates vary with gap size (Parsons et al. 1994) and differ between woodland canopies and interspaces (Padien and Lajtha 1992). The intermingling of different gap sizes within spatially complex ecotones (Gosz 1993, Risser 1995) and consequently the juxtaposition of different nutrient processing rates could favor one phase of vegetation or the other, depending upon the spatial context and gap size. Similarly, models of solar radiation influx based on three-dimensional canopy models (Rich et al. 1993) show an abrupt coalescence of shadows at moderate tree densities and thereby creation of a positive feedback to affect soil moisture content (Wilcox 1994) and to promote tree recruitment in the shade (Padien and Lajtha 1992). Seasonal changes in sun angle interact with canopy density to alter the ratio of monthly to annual variation in actual evapotranspiration (AET) throughout an ecotone, thereby favoring conifers or grasslands (Frank and Inouye 1994) depending upon location. Shifts in conditions that favor one vegetative phase or the other are related both to ecotone geometry and to edaphic and demographic conditions at each point.

Many geometrical properties of complex spatial patterns change suddenly with density and have been studied on random maps created on a lattice of cells (Stauffer 1985). Although the scaling properties of percolation maps are independent of the lattice geometry (Zallen 1983) we consider a square lattice because it corresponds to the raster geometry of digital images commonly used in geographic information systems.

By definition, a "uniform percolation map" is created by choosing a probability $0 < p \leq 1$ and then classifying each cell as "occupied" with probability p or "unoccupied" with probability $1 - p$; the state of

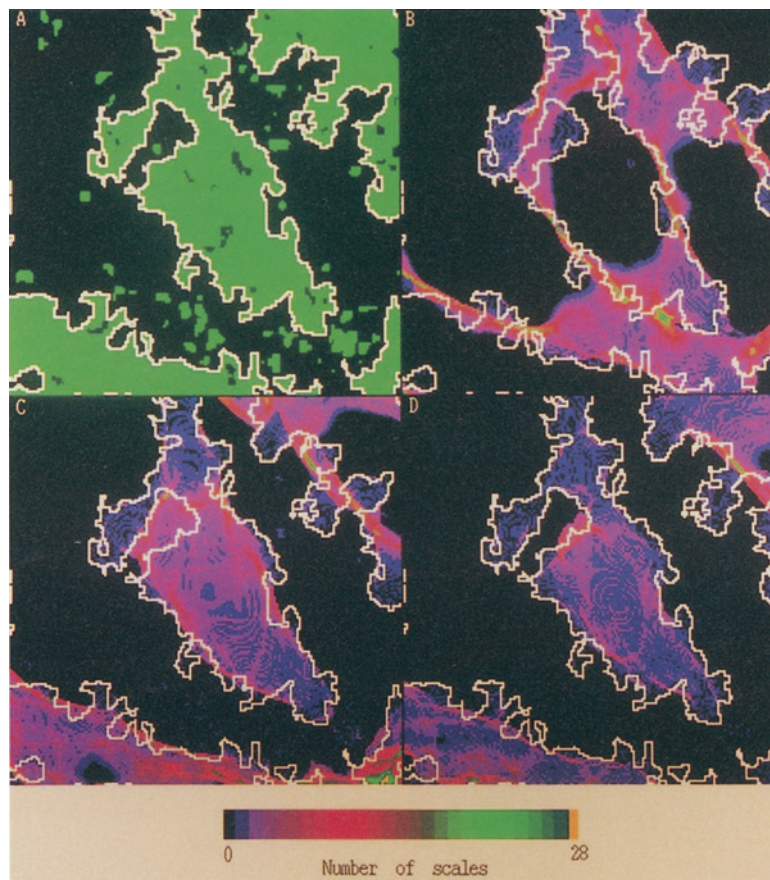
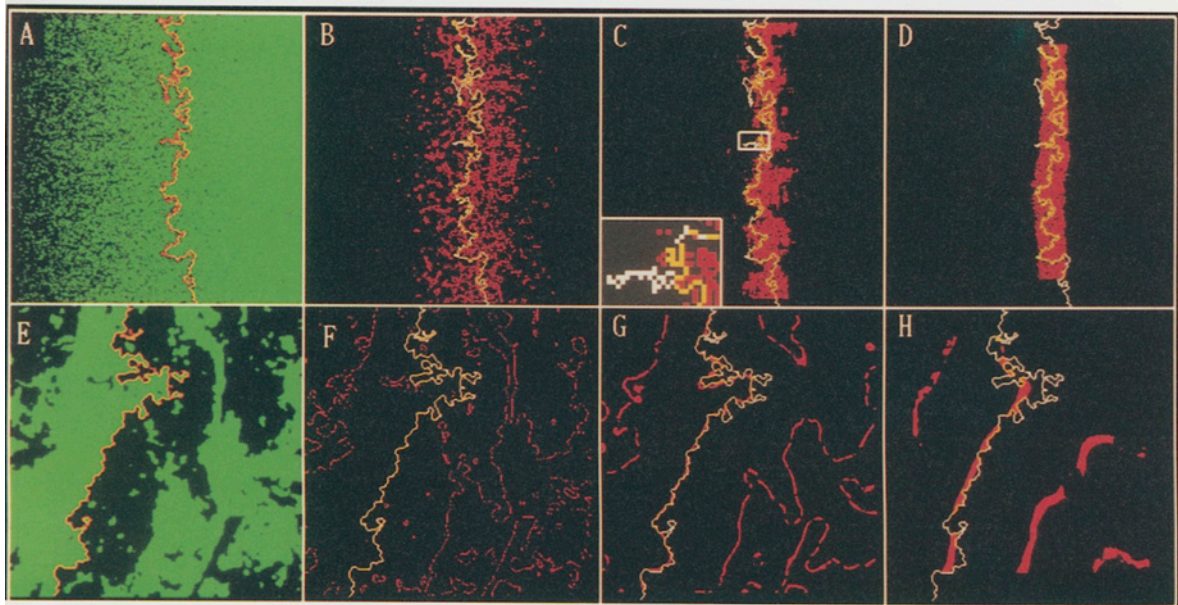


PLATE 2. Association between the hull and various local densities (proportions of cells occupied). (A) Classified image showing trees (green) and grassland (black). (B, C, D) Hulls (white) of tree clusters and the number of scales (windows of size $0.006 \text{ ha} \leq L \leq 2.48 \text{ ha}$) at which local densities of 0.50, 0.5928, and 0.70 (each $\pm 1\%$), respectively, were detected.

each cell is independent of the state of other cells (Gardner et al. 1987). A spatial phase transition occurs at a critical density of occupied cells, p_c , at which clusters of occupied cells coalesce to form at least one cluster that spans the width of the map. Such a cluster is called a “spanning” or percolation cluster (Stauffer 1985, Orbach 1986). [The term “percolation” refers to the potential for liquids or particles to move through highly connected sets of cells, as when water percolates through porous media.]

Spanning clusters alter diffusion (Orbach 1986, Johnson et al. 1992) by enabling organisms to traverse a landscape at p_c without leaving the cluster of connected cells. In the absence of a lattice, points can be considered neighbors if a process such as dispersal effectively links them. For example, tree density in piñon-juniper woodland shifts the competitive balance between two species of chipmunks (Brown 1971). At low tree densities, the more terrestrial and aggressive *Eutamias dorsalis* dominates, whereas the competitive advantage shifts abruptly to the more arboreal and social *Eutamias umbrinus* when tree density and size produce interlocking, or percolating, branch networks. In general, density alters interactions with predators or mates, if for example diffusion rates modify predation success (Murray and Mimura 1978) or the chance of finding mates during a mating season (Allee 1938, Bronstein et al. 1991).

Application of phase transition theory to landscapes is complicated by spatial variation in the probability of observing a particular vegetation type, as where forest cover increases with elevation. Whereas inspection can be used to estimate p_c on uniform maps, a different strategy is needed when underlying probability gradients are unknown. For example, a strip of forest along a river could form a spanning cluster even when the map as a whole has low forest coverage. In contrast, a small region that is above the critical probability may be an island in a sea of low probabilities; no spanning cluster would occur even though an ecologically meaningful environmental transition had occurred. Although the details of spatial phase transitions are well established for systems with known variations in p (e.g., Chopard et al. 1989, Roux and Guyon 1991, Margolina and Rosso 1992), we developed methods for situations with unknown spatial distributions of p .

We extended the concept of percolation to gradients by constructing “gradient percolation maps” (Feder 1988) in which p varied linearly from left to right but with a constant value within a column (Plate 1A). Gradient percolation maps provide simple models of landscapes in which probabilities vary spatially. The known gradients enabled experimental validation of our methods.

Analyses of percolation maps focus on “clusters” of occupied cells and their occupied neighbors. Various neighborhood rules can be defined with consequences for the geometrical properties of the clusters (Fig. 1).

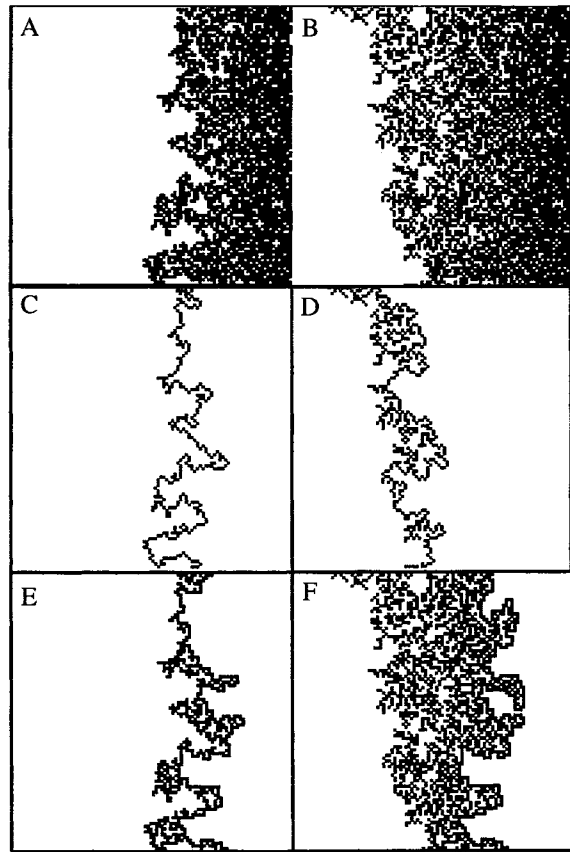


FIG. 1. Comparisons of spanning clusters, accessible edges, and hull edges based on 5-cell (left column) and 9-cell (right column) neighborhoods. For comparison, all panels were obtained from analyses of the same gradient percolation map with probabilities of occupied cells ranging from 0.1 to 0.9 (left to right) along the abscissa. (A) Spanning cluster (black) using the 5-cell neighborhood; (B) spanning cluster (black) using the 9-cell neighborhood; (C) accessible edge (black) of the cluster in panel A; (D) accessible edge of the cluster in B; (E) hull edge of the cluster in A; and (F) hull edge of the cluster in B.

Here, we consider two neighborhood definitions: the Moore 9-cell neighborhood, for which occupied cells can have neighbors in any of the eight vertical, horizontal, or diagonal directions, and the 5-cell von Neumann neighborhood, for which neighbors exist only in the four cardinal directions. The expected value of p_c depends on both the lattice geometry (e.g., square, triangular, hexagonal) and the neighborhood rule used to identify clusters of occupied cells (Zallen 1983, Stauffer 1985). The von Neumann rule gives $p_c = 0.59274$ while the Moore neighborhood applied to clusters on square lattices gives $p_c = 0.407 = 1 - 0.59274$ (Stauffer 1985). The apparent arbitrariness of $p_c = 0.5928$ relates remarkably well to the 61% cover threshold used by the U.S. Department of Agriculture Forest Service to classify woodlands and to a threshold of 60% canopy cover detectable by a canopy structural index

derived from remotely sensed Thematic Mapper images (Fiorella and Ripple 1993). These are coincidental similarities with the theory and would be homologous only if clusters were identified on a square lattice by the von Neumann rule.

A formal characterization of spatial phase transitions includes analyses of systems near a phase transition. In general terms we expect geometrical properties of the system to vary as a power of density near the critical density. A general scaling relation, characteristic of spatial phase transitions, is:

$$Q = |p - p_c|^\kappa, \quad (1)$$

where κ is a scaling exponent and Q is a quantity such as the probability that a cell belongs to the spanning cluster, the average size of clusters that do not contact the edge of the map, or the average squared distance of points within a cluster from the center of cluster mass (Grimmett 1989, Cresswick et al. 1992). Theoretical scaling exponents for these quantities on uniform percolation maps are $\beta = 5/36$, $\gamma = 43/18$, and $\nu = 4/3$ (Kesten 1987), respectively. Moreover, the exponents of the power laws satisfy the equality (Gould and Tobochnik 1988):

$$2\beta + \gamma = 2\nu. \quad (2)$$

Thus, evaluation of spatial phase transition theory: (1) requires the estimation of a critical density at which the phase transition occurs, (2) illustrates the power-law behavior we expect for many natural patterns (Mandelbrot 1982) as the critical density p_c is approached, and (3) provides numerical values for exponents that are expected for random maps. Exponents in the power laws are accurately estimated by techniques that adjust for the use of finite-sized maps (Reynolds et al. 1980, Gould and Tobochnik 1988).

Remarkably, the scaling exponents are identical for percolation maps formed on square, triangular, hexagonal, and dendritic lattices (Zallen 1983) and when either five-cell von Neumann or nine-cell Moore neighborhoods are used on square lattices (Gould and Tobochnik 1988). The consistency of the scaling exponents relates to the notion of a "universality class," which contains phenomena with disparate outward appearances but demonstrably similar statistical properties characterized by exponents. The universality concept has not been used in ecology but has potential to interrelate many phenomena much as Rosen (1989) suggested.

Thus, the theory of spatial phase transitions provides a series of hypotheses regarding the geometry of ecotones. First, estimation of a critical density is necessary to test the theory. Second, further support requires demonstrations of power law behavior near p_c . Third, statistical similarity between the observed and theoretical exponents would provide stronger evidence. Finally, an internally consistent geometry would be inferred

from empirical exponents that satisfy the scaling law, Eq. 2.

The goals of this paper are to: (1) test two alternative types of patch edges as indicators of the critical density on gradient, rather than uniform, percolation maps; (2) evaluate the consequences of two alternative cluster identification rules for use in the estimation of p_c ; (3) estimate p_c for real landscapes for which the underlying probability gradients are spatially complex and unknown; and (4) test that the empirical critical density equals the theoretical value. Future papers will use these results to extend percolation theory to landscapes in which probabilities vary spatially.

METHODS

Study area

Piñon-juniper woodlands cover $\approx 27 \times 10^6$ ha of the U.S. West (West 1984) and 7.81×10^6 ha in New Mexico, which has more area occupied by woodlands than any other state (Little 1977). Aerial photographs of woodlands and grasslands show high contrast between land cover classes and enable classification of imagery into two phases analogous to the occupied (woodland) and unoccupied (grassland) cells of percolation maps. The woodlands are of economic importance as rangeland and as sources of fuelwood and piñon pine nuts. Central New Mexico resides at the junction of several biomes that constitute the major floristic regions of the Southwest, i.e., Great Basin Shrubland, Montane Coniferous Forest, Shortgrass Prairie, Chihuahuan Desert, and Mogollon Woodland (McLaughlin 1986, Franklin et al. 1990). Thus, a sufficiently large pool of species exists in the region to enable rapid ecological responses to climate fluctuation or to changes in land use. Extensive and intensive drought in the 1950s produced rapid changes in community composition. For example, the lower elevation contour of the *Pinus edulis* range increased 100 m in elevation (Betancourt et al. 1993) and can be verified by analyses of terrain data and imagery used here (B. T. Milne, unpublished data). Rough terrain creates many ecotones in the study area.

Many factors regulate the distribution of piñon-juniper woodlands in southwestern landscapes. Relevant factors include glaciation (Van Devender and Spaulding 1979), latitudinal gradients in upper atmospheric circulation patterns (cf. Mitchell 1976), teleconnection of climate fluctuation (Neilson 1986, Sheaffer and Reiter 1985), elevation and massif size (West et al. 1975), slope aspect (Lymbery and Pieper 1983), soil type, grazing, fuelwood gathering, and wildfire (Jameson 1987). Alternative explanations for the distribution of woodlands can be based on water availability (e.g., Stephenson 1990, Frank and Inouye 1994), which is controlled by incident energy, precipitation, and soil properties (Eagleson and Segarra 1985). The controlling factors vary temporally and spatially over several

orders of magnitude (Woodward 1987), leading perhaps to nonequilibrium spatial distributions of the woodlands relative to the prevailing climatic, edaphic, and land-use conditions (Betancourt 1987, West and Van Pelt 1987).

We selected the U.S. Geological Survey Sandia Park quadrangle (35°7' N latitude, 106°15' E longitude) in New Mexico, USA for study. Elevation ranges from 1866 to 2408 m (mean 2071 m). Mean annual precipitation and temperature are 48.6 cm and 10°C, respectively (1939–1975). Extreme mean monthly temperatures are –1°C (January) and 21°C (July; Gabin and Lesperance 1977). Soils are shallow to deep, well-drained, very cobbly to silty clay loam, calcareous, and mildly to moderately alkaline (Hacker 1977). The area is underlain by undifferentiated Precambrian gneiss and schist, containing quartzite, amphibolite, and pegmatite, with Pennsylvanian fossiliferous limestone, shales, and sandstone, topped by Cretaceous and Quaternary alluvia (Kelley 1975). Land is primarily privately held and bounded on the west by the Sandia Mountains managed by the Cibola National Forest (Anonymous 1978). Land uses include ranching, fuel-wood production, recreation, and housing.

Imagery

Maps of woodlands and grasslands were made from digitized panchromatic aerial photographs (U.S. Soil Conservation Service aerial photography for 1935, 1:40 000 scale). Images were scanned at 113 dots/cm using an eight-bit Hewlett-Packard Scanjet IIc flatbed scanner. Image files were transferred from the scanned TIFF format to the VIFF format of the Khoros system (Rasure and Williams 1991, Konstantinides and Rasure 1994) and then to ASCII format for input to the Grass4.1 geographic information system (GIS), in which scanned images were combined into a mosaic and geographically rectified to the Universal Transverse Mercator coordinate system. The panchromatic scanned images were automatically classified into two classes corresponding to wooded areas and grasslands by *k*-means cluster analysis (Tou and Gonzalez 1974: 94). On panchromatic images, the *k*-means algorithm classifies pixels according to brightness while minimizing the root mean square error when assigning pixels to one of the *k* = 2 classes.

Resolution test

A definitive characteristic of fractals (e.g., ecotones; Milne 1991) is that they exhibit statistical self-similarity when viewed at different scales (Mandelbrot 1982); there is no single best scale at which to study fractals, and geometrical properties vary predictably with the scale of measurement. Thus, in theory, statistical characterizations of fractals, such as fractal dimensions or scaling exponents (Peitgen and Saupe 1988), should be independent of the scale at which the measurement is made. In practice however, empiricists

must represent spatial data at some finite resolution and on a finite-sized lattice. Since our analyses of piñon–juniper ecotones were based on measures related to fractal geometry, we used an independent fractal method to test whether the analyses of woodland geometry were sensitive to the resolution at which aerial photographs were scanned. We designed a factorial experiment to compare scanning density (i.e., pixels/cm), tree cover (*p*, here the probability that a given cell is occupied by trees), and the interaction between the two as they affected fractal characterizations of the images.

For the resolution test we scanned an aerial photograph taken over Sandia Park in 1935 at three resolutions: 39, 79, and 157 dots/cm. The original photograph was ≈1:40 000 scale, so pixels on the scanned images corresponded to 10, 5, and 2.5 m on the ground. The panchromatic (color-scale) digital images were automatically classified by the *k*-means cluster analysis into two classes corresponding to wooded areas and grasslands. Classification accuracy was checked by comparing the classified images to the aerial photographs. The three digital images were subdivided into 96 subimages that measured 2.5 × 2.5 cm. The total number of cells in each subimage varied according to the scanning resolution. To ensure independence we randomly selected one of the three scanning resolutions for each subimage location.

Two analyses were performed on each subimage. The first was simply a measurement of the proportional tree cover, *p*. The second analysis consisted of obtaining scaling exponents for various moments of the *P*(*m*, *L*) distribution (Peitgen and Saupe 1988, Milne 1991, 1992), which describes the probability *P* of observing *m* woodland cells within a window *L* cells wide. The distribution was obtained at several values of *L* by counting tree cells within overlapping windows centered on tree cells. The *P*(*m*, *L*) distribution has moments $M^q(L)$ indexed by an integer $-\infty < q < \infty$ that describes the configurations of cells within the windows, i.e., moments indexed by $q < 0$ characterize the occurrence of sparsely populated windows and moments indexed by $q > 0$ characterize locally dense windows. Nine moments were analyzed for $-4 \geq q \geq 4$. For each value of *q* we computed a scaling exponent D_q from $[M^q(L)]^{1/q} = kL^{D_q}$ as a measure of the scale dependence of the woodland pattern (Milne 1992); because the scaling relation is not defined for $q = 0$ we followed Voss (1988) and estimated D_0 as the slope of $S(L) \approx \ln L$ where $S(L) = \sum_m \log mP(m, L)$. In the absence of resolution effects and after controlling for *p*, we expected the exponents to be the same regardless of resolution.

Detection of critical density on gradients

Tree cover varies strongly with elevation (West 1984). Rough terrain creates an irregular surface of potential tree cover and *p* varies with spatial location.

This contrasts with uniform percolation maps (e.g., Orbach 1986), for which p_c can be assessed by comparing maps across a range of densities and finding the density at which the phase transition occurs, e.g., Gould and Tobochnik (1988). Limited theoretical investigations of percolation fronts on gradient maps have been made but all rely on known probability gradients. Consequently, we developed a new procedure to estimate p_c on empirical maps for which the underlying probability surface was unknown.

Two alternative indicators of the critical density on gradient percolation maps have been proposed, namely the "accessible edge" and the "hull edge" of percolation clusters (Grossman and Ahrony 1986, 1987, Feder 1988). The accessible edge is the set of outermost cells of the spanning cluster (Fig. 1C, D). The hull edge includes the accessible edge plus occupied cells with interior edges that can be accessed by crossing the accessible edge where its cells touch diagonally (Fig. 1). The interior margin of the hull is limited by the set of cells that touch along a common edge (Fig. 1E, F). On gradient percolation maps, which we use as simple models of landscapes, the hull and accessible edges of the spanning cluster appear approximately where the nominal density = p_c . To identify accurate indicators of the critical density, we tested whether the neighborhood rule interacts with the type of edge in estimations of p_c on gradient percolation maps.

Our technique of using the hull and accessible edges to estimate the critical densities of occupied cells on gradient percolation maps was stimulated by geometric measure theory (Morgan 1988) and by observations, on gradient percolation maps, of the scale-dependent association of the edges with local densities of 59.28% of cells occupied (Plate 1). We assessed local density by passing a sliding window of a given size over a gradient percolation map. We counted the number of occupied cells in each window, divided by the area of the window, and mapped the center point of the window in red (Plate 1B–D, F–H) if the density was within 5% of 59.28%. Preliminary observations showed that the locations at which critical densities were observed on random maps within small windows spanned a wider range of the abscissa than the locations identified by large windows (Plate 1B, C, D). This suggested that there are many opportunities for the edges to visit critical densities at fine scales. Fluctuations in the edges could be explained by local variations in density. We also noticed that edge cells coincided exactly with critically dense locations at some scales while other edge cells coincided at yet other scales (Plate 1F, G, H). Thus, the appearance of the critical density at a variety of scales suggested a multiscale approach to estimating the critical density on gradient percolation maps.

By definition, a cluster edge is formed from a contiguous series of occupied cells. This implies that the small convolutions of the edge are controlled by critical densities at fine scales while large convolutions are

controlled by broad scale variation in density, i.e., by definition there must be an unbroken field at p_c across the map through which the edge meanders. Thus, we envisioned the existence of a field of critical densities that could be detected at each scale. We hypothesized that the edges indicative of phase transitions should be restricted to domains in which critical densities occur. Conversely, the edges should be absent from places that lack the critical density. Specifically, we assumed that the critical density is constant over a range of scales and that tree cover, and presumably the ecological factors that control it, vary among arbitrarily sized subregions of the map. Under these assumptions there is no a priori reason to measure density at one particular scale. Rather, the general goal of the analysis is to assess the density of occupied cells at a variety of scales and determine which density (measured at many scales) has the highest association with the edge of large clusters.

Specifically, we inspected the map of tree cells with a series of square sliding windows of various sizes ranging from windows of 9 cells to windows 1/9th the area of the map. Within each window we divided the number of tree cells by the window area and mapped the center of the window if the observed tree density was within 1% of a selected value, i.e., a candidate critical density. After all window sizes had been used, we counted the number of locations where both the edge and the candidate density had been observed. We predicted that the co-occurrences would be highest when the critical density equalled the candidate density.

Assessment of hull and accessible edges with 5-cell neighborhoods ($p_c = 0.5928$).—We constructed a series of gradient percolation maps to compare the ability of the accessible and hull edges to detect a known value of p_c . To study the effect of map size, we made gradient percolation maps with widths of 128, 256, and 512 cells for studies of the accessible edge and widths of 128 and 256 cells for the hull edge. After a pilot study of the hull showed a striking nonlinear increase in the association between edges and the candidate densities near p_c , we selected target densities of 0.57, 0.5928, and 0.62 occupied cells per grid cell and created 18 replicate maps for each combination of edge type, map size, and target density. Both types of edges were constructed for clusters identified by the von Neumann neighborhood rule with an expected $p_c = 0.5928$ (Zallen 1983).

We sought further evidence for the accuracy of the technique from a second, independent, multiscale analysis of the woodland maps. Following our early observation (Plate 1) we conjectured that the critical-density estimation technique worked because the hull edge is necessarily constrained to occur at the critical density at ≥ 1 scale. To test this idea we rendered the original woodland map at successively coarser resolutions and then examined the relation between the hull and the

TABLE 1. Analysis of variance for the effect of tree cover, p , and scanning resolution on the scaling experiment of the first moment of the $P(m, L)$ distribution.

Source	df	MS	F	P
Model	21	0.01832	6.85	0.0001
p	7	0.05174	19.35	0.0001
Resolution	2	0.00376	1.41	0.2517
$p \times$ Resolution	12	0.00122	0.46	0.9335
Error	74	0.00267		

coarser renditions of the map. The rescaling process was a renormalization of the original map (Gould and Tobochnik 1988, Cresswick et al. 1992, Milne and Johnson 1993). Spatial renormalization is the process of rendering a map at a new resolution while preserving some particular geometrical property (Cresswick et al. 1992). Here, we applied the percolation rule that maintains the percolation structure of a map under successively coarser rescalings (Gould and Tobochnik 1988). The procedure entails inspecting blocks of 2×2 cells to find combinations of occupied (tree) cells that form continuous paths vertically or horizontally across the block (Gould and Tobochnik 1988). Percolation within a block is assured if there are two occupied cells adjacent in any one of four rectilinear (but not diagonal) configurations, or any of four configurations containing three occupied cells, or the configuration with four occupied cells. At each successive rescaling, blocks containing any one of these configurations were designated "occupied," thereby creating one cell where there had been four. We chose the percolation renormalization rule because it preserves the percolation geometry by diminishing occupied cells at low densities and amplifying those in locally dense regions. We hypothesized that if the hull necessarily occurs at densities near p_c at several scales simultaneously, then the original hull would remain embedded within the hull of the renormalized map as it was rescaled to 1/16 and 1/64 the resolution of the original.

Assessment of $p_c = 0.407$ from 9-cell neighborhoods.—As a final test, we applied the multiscale technique to spanning clusters of gradient percolation maps that had been identified by the 9-cell Moore neighborhood, i.e., both orthogonally and diagonally adjacent occupied cells. We expected that whatever edge was an accurate indicator under the 5-cell neighborhood rule would also be an accurate indicator if challenged with a different expected value for p_c .

Measurement of critical density on empirical maps

After confirming that the hull was an accurate and precise indicator of the critical density under the 5-cell rule, we used the hull to estimate p_c from classified aerial photographs of woodland. Given that real landscapes have much more complex vegetation patterns than the simple monotonic random gradients used in

the evaluation of our methodology, we expected that undulations in terrain could create isolated high-elevation regions with tree densities $> p_c$, i.e., there may not be a spanning cluster despite the existence of critical densities within subregions of the map. Thus, complex density gradients required a generalization of the concept of "spanning cluster." The spanning cluster of uniform percolation maps not only spans the entire map, by definition, but also is the largest cluster on the map. Thus, one possibility was to generalize to more complex maps by analyzing the hulls of unexpectedly large clusters. Given the bias in estimates of other fractal edge parameters such as the area-perimeter fractal dimension obtained from clusters with < 481 cells (Milne 1991), we required that "large" clusters contain ≥ 500 cells. We mapped the hulls of such clusters and then searched for the local density that maximized the association with the edge.

We replicated the study for maps with 65, 101, and 201 cells on a side (i.e., 2.72, 6.58, and 26.1 ha, respectively) selected from the composited aerial photographs of Sandia Park taken in 1935; each map was used for one estimate of the association with the edge. By studying several map sizes we expected to identify a threshold map size below which random processes of dispersal, establishment, and mortality create ecotones at $p_c = 0.59$. Larger maps had the potential to exhibit greater contagion due to the dominant role of terrain as a control of tree cover. Thus the null hypothesis was that $p_c = 0.5928$ for maps of all sizes.

RESULTS

The main result from studies of gradient percolation maps was that the hull of large clusters formed by the von Neumann rule accurately and precisely identified the theoretical critical density of 0.5928 of cells occupied while the accessible edge of clusters formed by the Moore rule accurately identified the theoretical critical density of 0.407 of cells occupied. Identification of clusters of trees from aerial photographs by the von Neumann rule and use of the hull edge yielded an estimated critical density of 0.5928 or 0.60 of cells occupied. Below we address the specific considerations for each analysis.

TABLE 2. Summary of ANOVA to test for an effect of density of cells occupied by tree canopies (p), scanning resolution, and the interaction of p and resolution on the scaling exponents for each of the moments q of the $P(m, L)$ distribution.

Source	Moments (q)								
	-4	-3	-2	-1	0	+1	+2	+3	+4
p	NS	NS	NS	NS	***	***	***	***	***
Resolution	NS	NS	NS	NS	NS	NS	NS	NS	NS
$p \times$ Resolution	NS	NS	NS	NS	NS	NS	NS	NS	NS

*** $P < 0.0001$.

NS, not significant.

TABLE 3. Analysis of variance of the rate of coincidence between the accessible edge of the percolation cluster defined using the 5-cell neighborhood rule, the local density of occupied cells ($p = 0.57, 0.5928, \text{ and } 0.62$), and map extent (128, 256, and 512 cells wide) as measured on monotonic gradient percolation maps.

Source	df	MS	F	P
Model	8	0.4536	56.90	0.0001
Local density	2	1.3965	175.17	0.0001
Map extent	2	0.2607	32.70	0.0001
Density \times extent	4	0.0786	9.86	0.0001
Error	151	0.0080		
Corrected total	159			

Resolution test

There was neither an effect of scanning resolution nor an interaction of scanning resolution and density p on the scaling exponents for each of the nine statistical moments included in the resolution analysis (Tables 1 and 2). A density effect on moments with $q > 0$ (i.e., moments that characterized relatively dense regions of the maps) was found for densities > 0.60 of cells occupied (Table 2), consistent with the expectations of a phase transition governed by a critical density. Thus, we elected to conduct the remaining analyses using a 2.5-m cell size, which approximated the diameter of juniper and pine crowns.

Assessment of $p_c = 0.5928$ and 5-cell neighborhoods.—We used monotonic gradient percolation maps to compare the hull and accessible edges as indicators of the known critical density $p_c = 0.5928$ on maps of clusters created by the 5-cell von Neumann neighborhood rule. In an analysis of variance of the rate at which each edge type coincided with local densities of 0.57, 0.5928 and 0.62 of cells occupied, there was a significant interaction between the type of edge and the local density ($F_{2, 204} = 58.11, P < 0.0001$). Consequently, separate ANOVAs were performed for each edge type. For a given map size, the accessible edge occurred with equal frequency at local densities of 0.57 and 0.5928 of cells occupied (Table 3, Fig. 2). In contrast there were significant differences in the coincidence rate of the hull at various local densities but no interaction between local density and map size (Table 4). Thus, the hull exhibited a maximal response at p_c , whereas the response of the accessible edge was an ambiguous indicator of the critical density.

Renormalization of the map to coarser scales demonstrated that the hulls of a high-resolution map remained embedded in the renormalized maps of woodland rendered at 1/16 and 1/64 the original resolution (Fig. 3). Occupied cells of the coarsely rendered maps (Fig. 3C, D) represented regions of either 16 or 64 of the original cells in which percolating configurations of occupied cells occurred, i.e., blocks that exhibited the phase transition configurations. Blocks without the percolating configurations were eliminated under successive renormalizations, e.g., some islands of trees

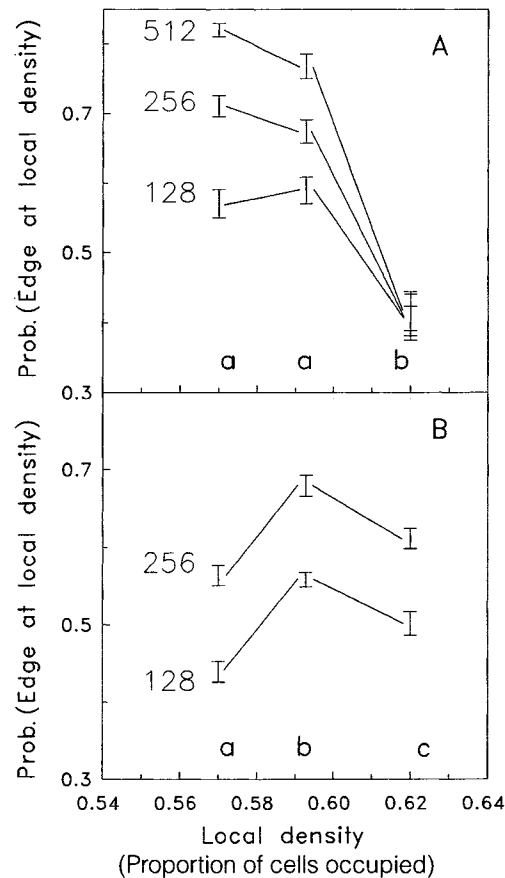


FIG. 2. Edge analysis of clusters formed by the 5-cell von Neumann rule on gradient percolation maps. Association of (A) accessible and (B) hull edges with local densities of 0.57, 0.5928, and 0.62 occupied cells per grid cell. The relations were measured on maps with 128, 256, or 512 cells per side. Vertical bars represent ± 1 standard error of the mean. Within an edge type and map size, local density treatments described by the same letter a, b, or c at bottom of panel were not significantly different ($\alpha = 0.05$).

and islands of grassland in Fig. 3B disappeared because they were not connected to larger clusters. Thus, the hull was largely restricted to subregions that contained the critical density at several nested scales.

Assessment of $p_c = 0.407$ with 9-cell neighbor-

TABLE 4. Analysis of variance of the rate of coincidence between the hull edges of percolating clusters defined by the 5-cell neighborhood rule, the local density of occupied cells ($p = 0.57, 0.5928, \text{ and } 0.62$), and map extent (widths of 128 and 256 cells), as measured on monotonic gradient percolation maps.

Source	df	MS	F	P
Model	5	0.1255	41.79	0.0001
Local density	2	0.1239	41.25	0.0001
Map extent	1	0.3787	126.09	0.0001
Density \times extent	2	0.0005	0.18	0.8345
Error	102	0.0030		
Total	107			

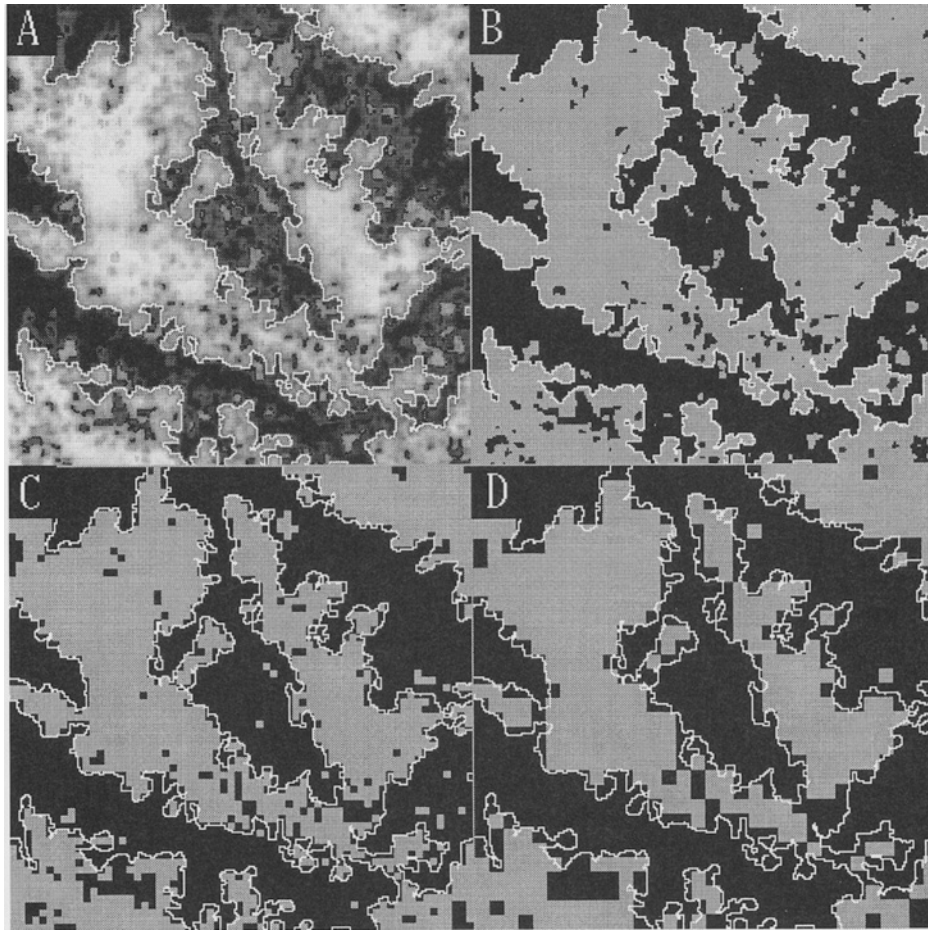


FIG. 3. Correspondence between the hull of a 41-ha empirical map and renormalized versions of the map. (A) digital image of woodland (dark tones) and grassland (light tones) with the hull (white) of clusters containing ≥ 500 cells, (B) binary classification of map A with hull (white) of the tree clusters (black), (C) renormalization of map B to 1/16 of the original resolution with the hull (white) overlaid at its original resolution, (D) renormalization to 1/64 resolution with the original hull (white).

hoods.—Surprisingly, we found a significant interaction between the type of edge and the neighborhood rule such that the accessible edge had a significantly higher probability of occurring at the theoretical critical density of $p = 0.407$ of cells occupied when clusters were identified by the 9-cell rule (Fig. 4, $F_{4, 149} = 540.01$, $P < 0.0001$). Given the interaction with edge type, we made separate analyses for each edge type to characterize the effects of map size and local density (Tables 5, 6). When applied to clusters identified by 9-cell neighborhoods, the accessible edge responded more strongly to local densities of the expected $p_c = 0.407$ on large maps (512^2 cells) than on small (interaction effect, Table 5, Fig. 4A). In contrast, the hull not only had a significantly weaker response at $p = 0.407$ but reached a maximal response at $p = 0.5928$, which is the critical density for 5-cell neighborhoods (Fig. 4B). Hulls exhibited neither an effect of map size nor an interaction between map size and local density

(Table 6). The accessible edge indicated the expected critical value under the Moore rule.

Measurement of critical density on empirical maps

On aerial photographs the hull occurred significantly more frequently at local densities of $p = 0.5928$ or 0.60 of cells occupied when small and medium size maps were used (Fig. 5A, B; effect of local density $F_{5, 185} = 12.5$, $P < 0.0001$). The multiscale maps showing the locations of densities of 0.50, 0.5928, and 0.70 occupied cells per grid cell illustrated the tendency for the hull to be associated with the critical density (Plate 2). Consistent with a phase transition, the maps illustrated shifts in the spatial distribution of locations where the various local densities were found. For example, when we used a local density of 0.50 occupied cells per grid cell, the bulk of occurrences were at the interface between grassland and woodland; the woodlands seldom contained these locations (Plate 2B). The

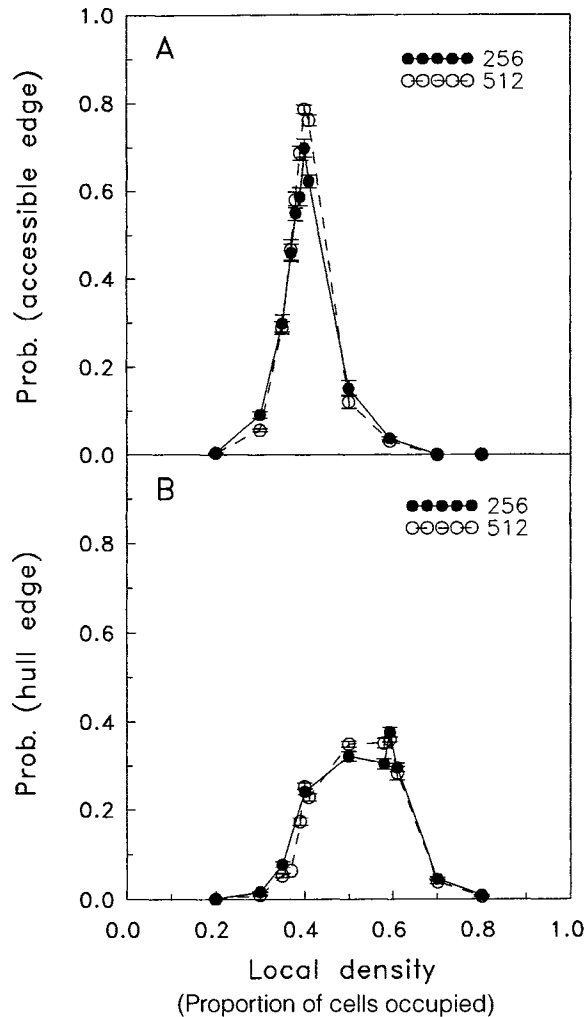


FIG. 4. Occurrence of accessible and hull edges at multiple scales as functions of local density on spanning clusters of gradient percolation maps. Clusters were identified by the 9-cell rule. (A) Probability that the accessible edge was coincident with various local densities at two map sizes. (B) Probability of hull occurring at various local densities for two map sizes. Vertical bars represent ± 1 SE of the mean.

occurrences shifted to locations within large woodland clusters when local densities $\geq p_c$ were mapped (Plate 2C, D). On large maps (26 ha) the local density of 0.5928 occupied cells per grid cell had the highest mean association with the hull (62%) but the hull was associated equally well with most of the local densities between 0.5 and 0.61 of cells occupied (Fig. 5C). One exception was a significantly higher association with 0.5928 compared to 0.585 of cells occupied (effect of local density, $F_{6,40} = 2.92$, $P = 0.019$, Tukey multiple comparisons test $\alpha = 0.05$). Thus, a critical density was poorly defined for large maps but equal to the theoretical value on small and medium maps.

In summary, the hull accurately identified the expected critical density when applied to clusters formed

TABLE 5. Analysis of variance of the rates of coincidence between the accessible edge and local density of occupied cells ($p = 0.37, 0.38, 0.39, 0.40, 0.41, 0.5928$) for maps 256 and 512 cells wide. Spanning clusters were defined by the 9-cell neighborhood rule on gradient percolation maps.

Source	df	MS	F	P
Model	11	0.6072	231.95	0.0001
Density	5	1.3014	497.16	0.0001
Map extent	1	0.0942	35.99	0.0001
Density \times extent	5	0.0155	5.93	0.0001
Error	105	0.0026		
Total	116			

by the von Neumann rule but the occurrence of the accessible edge with local densities of 0.5928 of cells occupied was affected by an interaction between local density and map size. However, the accessible edge was an accurate indicator of the critical density for clusters formed by the Moore rule, and its association with p_c increased with map size. Empirical maps of woodland exhibited a critical density equal to that predicted by the theory of spatial phase transitions.

DISCUSSION

The unexpected interaction between the neighborhood rule and the edge type has implications for the precise measurement of canopy coverage in studies of plant-environment relations. First, we note that the two accurate edges (Fig. 1D, E) shared similar geometric properties despite differences in construction. Apparently, application of the accessible edge to von Neumann clusters underestimated the critical density because the edge was too narrow and tended to occur at densities $< p_c$. Conversely, application of the hull to Moore clusters overestimated the critical value (Fig. 4B) because the hull was too wide (Fig. 1F).

The demonstration of two accurate and precise indicators of two different critical densities suggested that a given landscape could be mapped by both neighborhood rules. Then, contours would be revealed where the woodland was at a particular local density. The potential to partition canopy cover within a narrow range has potential application in the calibration of remotely sensed imagery obtained from satellite sensors (e.g., Zhu and Evans 1994).

TABLE 6. Analysis of variance of the rates of coincidence between the hull edge and local density of occupied cells ($p = 0.37, 0.38, 0.39, 0.40, 0.41, 0.5928$) for maps 256 and 512 cells wide. Spanning clusters were defined by the 9-cell neighborhood rule.

Source	df	MS	F	P
Model	6	0.0493	88.29	0.0001
Density	4	0.0735	131.51	0.0001
Map extent	1	0.00005	0.09	0.7636
Density \times extent	1	0.00203	3.63	0.0633
Error	44	0.00056		
Total	50			

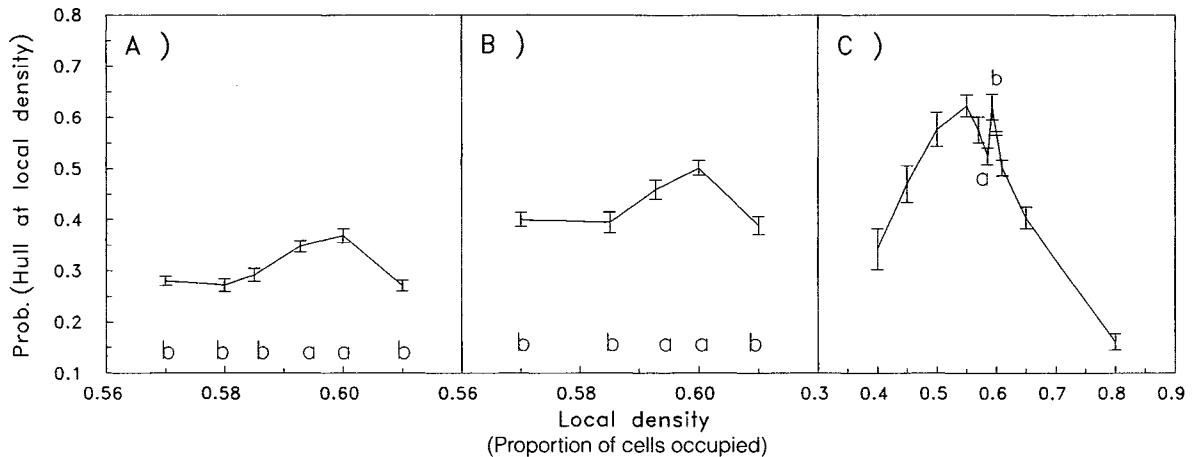


FIG. 5. Probabilities that the hull (5-cell neighborhood) occurred at local densities near 0.5928 measured on empirical maps of piñon-juniper woodland made from aerial photographs taken in 1935 in Sandia Park, New Mexico. (A) 2.72-ha maps, (B) 6.58-ha maps, (C) 26.1-ha maps. Densities with different lowercase letters were significantly different at $\alpha=0.05$. Comparisons among local densities in C were limited to the range 0.5–0.61; the one significant difference was between densities 0.5928 and 0.585. Vertical bars represent ± 1 SE of the mean.

Entire subregions of landscapes potentially contain edges indicative of phase transitions (Plate 2). In such regions, slight gains or losses of trees make it theoretically possible for an edge to move while remaining in parts of the landscape that are at the critical density at some scale or other. Thus, it is possible that under constant environmental conditions ecotones wobble stochastically across the landscape. Attempts to find landscapes that have experienced non-stochastic fluctuations in ecotone location, as expected in scenarios of climate change, should first identify regions at the critical density and then show that ecotones have moved beyond those regions. Multiscale maps of local density would provide geographic features analogous to confidence intervals and might satisfy Noble's (1993) recent criticism of ecotones as sites for monitoring climate change. For example, if increased temperatures were to decrease the water available for tree growth then some locations formerly with $p \geq p_c$ would switch to $p < p_c$. Thus, we would expect ecotones to escape from regions that were at critical densities before climate change. It would be useful to differentiate ecotone movements with respect to the scale at which the critical density occurred. Movements out of regions originally at p_c measured within small areas should occur more frequently than movements away from p_c mapped within larger areas because of the myriad interacting factors that control ecotones at fine scales (Gosz 1991). Presumably, fluctuations over small areas require weaker forcing functions than movements over broader areas. Enumeration of a hierarchy (Allen and Starr 1982) of environmental controls on ecotone location could be determined by partitioning the scales at which fluctuations occurred.

Multiscale maps of local tree cover (Plate 2) suggest that there are locations both within and outside of large

clusters, or similarly upslope and downslope from elevational limits, where sub-critical environmental conditions may occur. For example, given the interaction between elevation and slope aspect, trees at high elevations may or may not be in environments that promote densities associated with hull- or accessible-edge ecotones. Thus, attempts to calibrate species responses as "direct" functions (*sensu* Whittaker 1967, Austin 1985, Jongman et al. 1987) of elevation may inadvertently sample environments that are dissimilar from the environmental thresholds that separate two or more vegetative phases. Perhaps the precision with which hull and accessible edges indicate particular coverages can improve calibration efforts.

We expect the accessible (Moore) and hull (von Neumann) edges to be spatially separate or non-overlapping where the terrain represents shallow gradients in the environmental factors that control tree density. However, there are probably many places where steep environmental gradients occur, as with abrupt changes in soil texture or where elevation changes over short distances. In such cases we expect the accessible and hull edges (computed from 9-cell and 5-cell neighborhoods, respectively) to overlap because of the proximity of environmental conditions that produce canopy coverages of 40.7 and 59.3%. Thus, given the appropriate neighborhood rule, the hull and the accessible edges could be used to detect regions with shallow gradients. We illustrated this possibility (Fig. 6) along with the geometric measures of local densities to show two insights from this study. First, where the edges overlapped (Fig. 6B), the ecotones were ambiguous indicators of tree cover p and presumably of the environmental conditions associated with canopy coverages of 40 and 59%. This was apparent from the overlapping geometric measures of the two critical den-

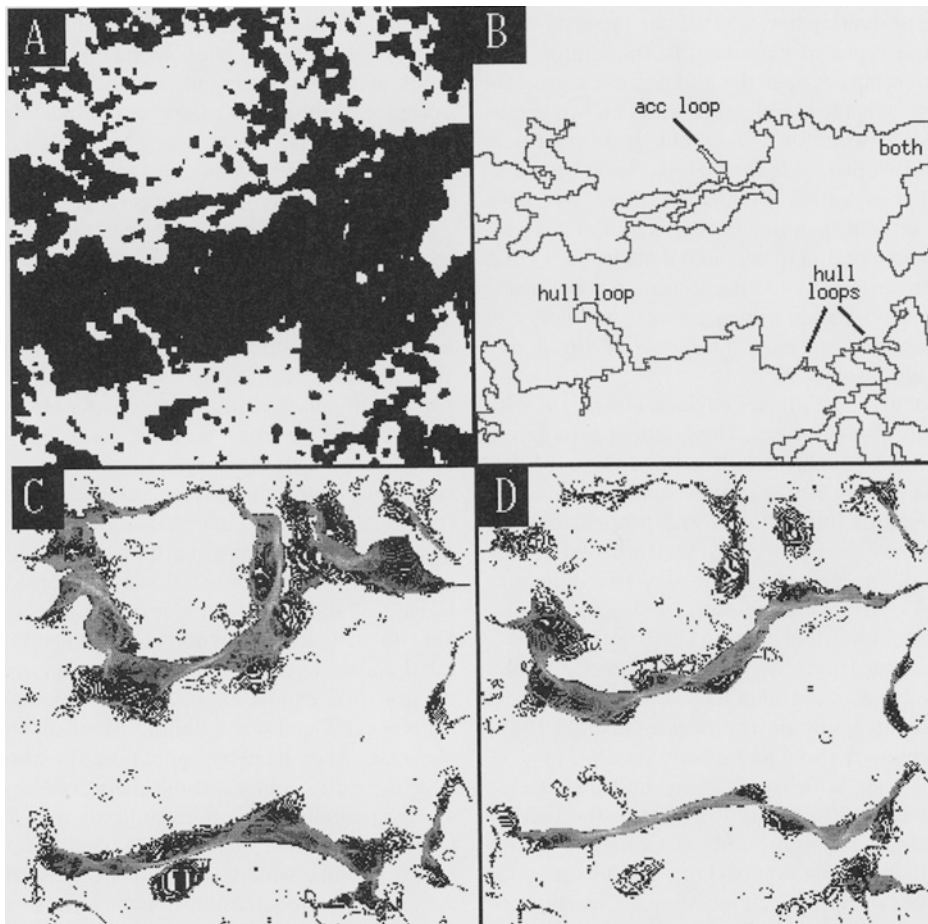


FIG. 6. Simultaneous mapping of the accessible edge and the hull. (A) 42-ha map of woodland (black) and grassland (white) from an image of Sandia Park, New Mexico, taken in 1935. (B) Accessible edge (indicative of 40% cover) and the hull (59% cover) of the spanning cluster of woodland as defined by the 9-cell rule for the accessible edge and the 5-cell rule for the hull. Closed loops, where one edge or the other makes a solitary excursion, are labelled. (C) Locations with local densities $p = 0.407 \pm 1\%$; shading proportional to number of scales (black = detection at 1 scale; number of scales increases with lighter tones). (D) Locations with local densities of $0.5928 \pm 1\%$.

sities (Fig. 6C, D). Second, attempts to calibrate the environmental conditions associated with 40% tree cover should be made where the accessible edge occurs alone, as it did in this example where a peninsula of woodland made an incursion into grassland, i.e., where the woodland cover was locally sparse. The loop of accessible edge occurred where the local density of occupied cells, $p = 0.407$, was high (Fig. 6C) while that for local density of 0.5928 was low. In general, the underlying probability gradient between grassland and woodland was steep at the 2.5-m resolution.

Neighborhood rules for the identification of clusters are in some sense arbitrary and therefore subject to modification. In general, a rule that involves more neighbors (e.g., 9-cell Moore rule) creates spanning clusters at lower densities because there are more opportunities for cells to be adjacent to one another. It would be advantageous to invent neighborhood rules with somewhat greater critical densities and then find corresponding

edges indicative of the respective critical density. This would enable regions to be identified where the local density varies gradually from 0.59 to 0.7, say, and thus avoid the same problem that exists when attempting to calibrate plant–environment relations where indicators of local densities of 0.4 and 0.59 overlap.

It is reasonable to use a geographic information system to relate the edges, say, to environmental conditions such as elevation, slope, and aspect from a digital elevation model (DEM), to remotely sensed images from coarser spatial scales, or to geographically explicit predictions of soil water flux. Calibration attempts should avoid gathering GIS data about either edge when both types of edge cells (2.5-m width) occur within the same 30-m DEM cell. Rather, estimates of environmental conditions associated with a particular percent cover should best be made where an edge is isolated from indicators of phase transitions at other critical densities.

The degree of overlap between the two types of edges implies several types of ecotones. In the simple case of complete overlap between the hull and the accessible edge, the ecotone is the visible edge between two patches, as between a woodlot and a field. In other cases, such as on a hillslope ranging from low-elevation grasslands to higher elevation woodlands, there will be a hull of the grassland spanning cluster, a hull of a woodland cluster, and a region in between that has both grass cells and tree cells at densities less than the critical value. Application of spatial phase transition theory to woodland ecotones suggested a richness of alternative ecotone configurations.

The static analysis of cluster edges is consistent with a dynamical view of ecotones. The gradient percolation literature (Chopard et al. 1989, Roux and Guyon 1991, Margolina and Rosso 1992) applies similar techniques to study moving diffusion fronts and propensities for movement. Ecosystem processes that are tied to the maintenance of the ecotone, such as water dynamics (Johnston 1993, Arris and Eagleson 1994), competition (Neilson 1993), or nutrient cycling (Parsons et al. 1994, Padien and Lajtha 1992), are modified directly by the geometry of the ecotone and thus a static treatment relates both to the regulation of processes (Turner 1989) and to the dynamics (Solé and Manrubia 1995).

Indeed, ecotones with overlapping hull and accessible edges may be less likely to move in the face of modest climate fluctuations. This is explained by invoking a continuous function $p(x)$ to describe the probability that trees occur at each location x . Clearly, ecotones between an agricultural field and a woodlot have a step function of $p(x)$ due to intensive management. Climate changes capable of decreasing $p(x)$ by 10% would not be discernible as a geographical shift of the woodlot edge because the locations at which $p = 0.59$ and $p = 0.407$ would remain coincident. However, a 10% change in $p(x)$ along a shallow gradient, as on a hillslope, would produce noticeable elevational shifts in the ecotone; the location of $p(x) = p_c$ would shift inversely with $\partial p(x)/\partial x$. Thus, areas with separate hull and accessible edges are candidates for visible ecotone responses to climate fluctuations.

Fractal indices such as scaling exponents of the $P(m,L)$ distribution were, within the boundaries of our experimental protocol, independent of image resolution. We conclude that the measures we used in our exploration of piñon–juniper ecotones represented attributes of the underlying spatial pattern of tree distribution and were not artifacts of our data collection methods.

An intriguing paradox results from the application of gradient percolation theory to landscapes. On one hand, the association of critical densities with geometric features such as hulls and accessible edges is phenomenological and currently lacks a direct association with ecological mechanisms or environmental conditions. Many ecological observations are of this

sort and much of ecology is devoted to the construction of relations between phenomena and independent measures of the environment. On the other hand, the occurrence of the edges wherever the local density equals p_c indicates that the hull or accessible edges indicate locations where all relevant factors conspire to create the critical density. It is conceivable that in some cases a single factor creates an ecotone, as where differences in land use on either side of an ownership boundary produce different plant communities. However, in considering the geographic range of piñon–juniper woodlands, it is reasonable to assume that various factors, such as water availability (Neilson 1993), growing season length, onset of summer monsoonal moisture, inter-populational genetic variation, land use, accidents of establishment, fire history, or grazing pressures operate to various degrees from place to place and at each scale (Gosz 1991). Thus, many factors may create canopy coverages of 59% and the hull would be the best indicator of the effects of all such factors. This characteristic of indicating the combined effects of all relevant factors, known or unknown, imparts an unparalleled completeness to this particular environmental indicator. We expect that if environmental conditions such as AET and water deficit (Stephenson 1990) were measured over the geographic range of woodland wherever the hull occurred alone there would generally be a clear association with these predictors. However, attempts to calibrate such relations with local, rather than regional, data would probably be frustrated by idiosyncrasies of local conditions and environmental history. Thus, large residuals from calibrations made over the geographic range might indicate the presence of other factors that operate at finer scales.

Application of percolation theory to the study of ecotones revealed several novel empirical phenomena. Foremost were the multiscale density fields (Plate 2), which identify regions capable of containing edges indicative of critical densities. Overlap in the two types of edge that accurately and precisely indicate particular probabilities revealed locations of steep environmental gradients with implications for estimations of plant–environment relations. Moreover, multiscale analyses of woodlands indicated maximal hull responses at the critical density predicted by percolation theory, suggesting the appropriateness of this formalism for studies of ecotones. In general, percolation theory provides the rudiments of an a-priori theory of ecotones and may enable reproducible, objective applications in other landscapes.

ACKNOWLEDGMENTS

We appreciate the support of the NSF (grants BSR-9058136 to B. T. Milne and BSR-9107339 to B. T. Milne and A. R. Johnson) and the Electric Power Research Institute grant to B. T. Milne. David Breshears contributed to our understanding of ecological mechanisms associated with ecotones. The manuscript benefitted from comments by Craig Loehle, Bailian Li, Don DeAngelis, and an anonymous reviewer. Sevilleta LTER publication no. 75.

LITERATURE CITED

- Allee, W. C. 1938. *The social life of animals*. W.W. Norton, New York, New York, USA.
- Allen, T. F. H., and T. B. Starr. 1982. *Hierarchy*. University of Chicago Press, Chicago, Illinois, USA.
- Anonymous. 1978. Albuquerque, New Mexico surface management. United States Department of the Interior, Bureau of Land Management, Washington, D.C., USA.
- Arris, L. L., and P. S. Eagleson. 1994. A water use model for locating the boreal/deciduous forest ecotone in eastern North America. *Water Resources Research* **30**:1–9.
- Austin, M. P. 1985. Continuum concept, ordination methods, and niche theory. *Annual Review of Ecology and Systematics* **16**:39–61.
- Betancourt, J. L. 1987. Paleoecology of pinyon-juniper woodlands: summary. Pages 129–139 in R. L. Everett, editor. *Proceedings—Pinyon-Juniper conference*. U.S. Department of Agriculture Forest Service General Technical Report INT-215.
- Betancourt, J. L., E. A. Pierson, K. A. Rylander, J. A. Fairchild Parks, and J. S. Dean. 1993. Influence of history and climate on New Mexico piñon–juniper woodlands. Pages 42–62 in E. F. Aldon, and D. W. Shaw, editors. *Managing piñon–juniper ecosystems for sustainability and social needs*. Proceedings of a Symposium (April 26–30, Santa Fe, New Mexico). U.S. Department of Agriculture Forest Service, Rocky Mountain Forest and Range Experiment Station, General Technical Report RM-236, Fort Collins, Colorado, USA.
- Botkin, D. B., J. F. Janak, and J. R. Wallis. 1972. Some ecological consequences of a computer model of forest growth. *Journal of Ecology* **60**:849–872.
- Bronstein, J. L., P.-H. Gouyon, C. Gliddon, F. Kjellberg, and G. Michaloud. 1991. The ecological consequences of flowering asynchrony in monocious figs: a simulation study. *Ecology* **71**:2145–2156.
- Brown, J. H. 1971. Mechanisms of competitive exclusion between two species of chipmunks. *Ecology* **52**:305–311.
- Chopard, B., M. Droz, and M. Kolb. 1989. Cellular automata approach to non-equilibrium diffusion and gradient percolation. *Journal of Physics A* **22**:1609–1619.
- Cody, M. 1989. Discussion: structure and assembly of communities. Pages 227–241 in *Perspectives in ecological theory*. J. Roughgarden, R. M. May, and S. A. Levin, editors. Princeton University Press, Princeton, New Jersey, USA.
- Cresswick, R. J., H. A. Farach, and C. P. Poole, Jr. 1992. *Introduction to renormalization group methods in physics*. John Wiley and Sons, New York, New York, USA.
- DeAngelis, D. L., W. M. Post, and C. C. Travis. 1986. *Positive feedback in natural systems*. Springer-Verlag, Berlin, Germany.
- Domb, C., and J. L. Lebowitz. 1988. *Phase transitions and critical phenomena*. Volume 12. Academic Press, London, England.
- Eagleson, P. S., and R. I. Segarra. 1985. Water-limited equilibrium of savanna vegetation systems. *Water Resources Research* **21**:1483–1493.
- Feder, J. 1988. *Fractals*. Plenum, New York, New York, USA.
- Fiorella, M., and W. J. Ripple. 1993. Analysis of conifer forest regeneration using Landsat Thematic Mapper data. *Photogrammetric Engineering and Remote Sensing* **59**:1383–1388.
- Fortin, M.-J. 1994. Edge detection algorithms for two-dimensional ecological data. *Ecology* **75**:956–965.
- Frank, D. A., and R. S. Inouye. 1994. Temporal variation in actual evapotranspiration of terrestrial ecosystems: patterns and ecological processes. *Journal of Biogeography* **21**:401–411.
- Franklin, J. F., C. S. Bledsoe, and J. T. Callahan. 1990. Contributions of the long-term ecological research program. *BioScience* **40**:509–523.
- Gabin, V. L., and L. E. Lesperance. 1977. New Mexico climatological data. W.K. Summers and Associates, Socorro, New Mexico, USA.
- Gardner, R. H., B. T. Milne, M. G. Turner, and R. V. O'Neill. 1987. Neutral models for the analysis of broad-scale landscape pattern. *Landscape Ecology* **1**:19–28.
- Gosz, J. R. 1991. Fundamental ecological characteristics of landscape boundaries. Pages 8–30 in M. M. Holland, R. J. Naiman, and P. G. Risser, editors. *Role of landscape boundaries in the management and restoration of changing environments*. Chapman and Hall, New York, New York, USA.
- . 1993. Ecotone hierarchies. *Ecological Applications* **3**:369–376.
- Gosz, J. R., and J. H. Sharpe. 1989. Broad-scale concepts for interactions of climate, topography, and biota at biome transitions. *Landscape Ecology* **3**:229–243.
- Gould, H., and J. Tobochnik. 1988. *An introduction to computer simulation methods: applications to physical systems*. Part 2. Addison-Wesley, Reading, Massachusetts, USA.
- Grassberger, P. 1983. On the critical behavior of the general epidemic process and dynamical percolation. *Mathematical Biosciences* **63**:157–172.
- Grimmett, G. 1989. *Percolation*. Springer-Verlag, Berlin, Germany.
- Grossman, T., and A. Ahrony. 1986. Structure and perimeters of percolation clusters. *Journal of Physics A* **19**:L745–L751.
- Grossman, T., and A. Ahrony. 1987. Accessible external perimeters of percolation clusters. *Journal of Physics A* **20**:L1193–L1201.
- Hacker, L. W. 1977. Soil survey of Bernalillo County and parts of Sandoval and Valencia Counties, New Mexico. U.S. Department of Agriculture, Soil Conservation Service, Washington D.C., USA.
- Holland, M. M., P. G. Risser, and R. J. Naiman, editors. 1991. *Ecotones*. Chapman and Hall, New York, New York, USA.
- Jameson, D. A. 1987. Climax or alternative steady states in woodland ecology. Pages 9–13 in R. L. Everett, editor. *Proceedings—pinyon–juniper conference*. U.S. Department of Agriculture Forest Service General Technical Report INT-215.
- Johnson, A. R., B. T. Milne, and J. A. Wiens. 1992. Diffusion in fractal landscapes: simulations and experimental studies of Tenebrionid beetle movements. *Ecology* **73**:1968–1983.
- Johnston, C. A. 1993. Material fluxes across wetland ecotones in northern landscapes. *Ecological Applications* **3**:424–440.
- Jongman, R. H. G., C. J. F. ter Braak, and O. F. R. van Tongeren, editors. 1987. *Data analysis in community and landscape ecology*. Center for Agricultural Publishing and Documentation, Wageningen, The Netherlands.
- Kay, J. J., and E. D. Schneider. 1992. Thermodynamics and measures of ecological integrity. Pages 159–182 in D. H. McKenzie, D. E. Hyatt, and V. J. McDonald, editors. *Ecological indicators*. Volume 1. Elsevier Applied Science, London, England, and New York, New York, USA.
- Kelley, V. C. 1975. *Geologic map of Sandia Mountains area, New Mexico*. New Mexico Bureau of Mines and Mineral Resources, Socorro, New Mexico, USA.
- Kesten, H. 1987. Scaling relations for 2D-percolation. *Communications in Mathematical Physics* **109**:109–156.
- Konstantinides, K., and J. R. Rasure. 1994. The Khoros software development environment for image and signal processing. IEEE (Institute of Electrical and Electronics Engineers) *Transactions on Image Processing* **3**:243–252.
- Levin, S. A., and R. T. Paine. 1974. Disturbance, patch for-

- mation, and community structure. *Proceedings of the National Academy of Sciences* **71**:2744–2747.
- Levin, S. A., and L. A. Segel. 1985. Pattern generation in space and aspect. *SIAM (Society for Industrial and Applied Mathematics) Review* **27**:45–67.
- Little, E. L., Jr. 1977. Research in the pinyon–juniper woodland. In E. F. Aldon and T. J. Loring (technical coordinator). *Ecology, uses, and management of pinyon–juniper woodlands: proceedings of the workshop*. U.S. Department of Agriculture Forest Service General Technical Report **RM-39**.
- Lymbery, G. A., and R. D. Pieper. 1983. Ecology of pinyon–juniper vegetation in the northern Sacramento Mountains. *New Mexico State University Agricultural Experiment Station Bulletin* **698**.
- MacKay, G., and N. Jan. 1984. Forest fires as critical phenomena. *Journal of Physics A* **17**:L757–L760.
- Mandelbrot, B. B. 1982. *The fractal geometry of nature*. Freeman, New York, New York, USA.
- Margolina, A., and M. Rosso. 1992. Illumination: a new method for studying 3D percolation fronts in a concentration gradient. *Journal of Physics A* **25**:3901–3912.
- McLaughlin, S. P. 1986. Floristic analysis of the southwestern United States. *Great Basin Naturalist* **46**:46–65.
- Meakin, P. 1983. Diffusion-controlled deposition on fibers and surfaces. *Physical Review A* **27**:2616–2633.
- Milne, B. T. 1991. Lessons from analyzing fractal models to landscape patterns. Pages 199–235 in *Quantitative methods in landscape ecology*. M. G. Turner and R. H. Gardner, editors. Springer-Verlag, New York, New York, USA.
- . 1992. Spatial aggregation and neutral models in fractal landscapes. *American Naturalist* **139**:32–57.
- Milne, B. T., and A. R. Johnson. 1993. Renormalization relations for scale transformation in ecology. Pages 109–128 in R. H. Gardner, editor. *Some mathematical questions in biology: predicting spatial effects in ecological systems*. American Mathematical Society, Providence, Rhode Island, USA.
- Milne, B. T., M. G. Turner, J. A. Wiens, and A. R. Johnson. 1992. Interactions between the fractal geometry of landscapes and allometric herbivory. *Theoretical Population Biology* **41**:337–353.
- Mitchell, V. L. 1976. The regionalization of climate in the western United States. *Journal of Applied Meteorology* **15**:920–927.
- Morgan, F. 1988. *Geometric measure theory*. Academic Press, New York, New York, USA.
- Murray, J. D. 1984. On a mechanical model for morphogenesis: mesochymal patterns. Pages 279–291 in W. Jäger and J. D. Murray, editors. *Lecture notes in biomathematics*. Springer-Verlag, Berlin, Germany.
- Murray, J. D., and M. Mimura. 1978. On a diffusion predator model which exhibits patchiness. *Journal of Theoretical Biology* **75**:249–262.
- Neilson, R. P. 1986. High resolution climatic analysis and southwest biogeography. *Science* **232**:27–34.
- . 1993. Transient ecotone response to climatic change: some conceptual and modelling approaches. *Ecological Applications* **3**:385–395.
- Noble, I. R. 1993. A model of the responses of ecotones to climate change. *Ecological Applications* **3**:396–403.
- Odum, E. P. 1959. *Fundamentals of ecology*. W. B. Saunders, Philadelphia, Pennsylvania, USA.
- Ohtsuki, T., and T. Keyes. 1983a. Biased percolation: forest fires with wind. *Journal of Physics A* **19**:L281–L287.
- Ohtsuki, T., and T. Keyes. 1983b. Kinetic growth percolation: epidemic processes with immunization. *Physical Review A* **33**:1223–1232.
- O'Neill, R. V., A. R. Johnson, and A. W. King. 1989. A hierarchical framework for the analysis of scale. *Landscape Ecology* **3**:193–205.
- Orbach, R. 1986. Dynamics on fractal networks. *Science* **231**:814–819.
- Ouimet, C., and P. Legendre. 1988. Practical aspects of modelling ecological phenomena using the cusp catastrophe. *Ecological Modelling* **42**:265–287.
- Padien, D. J., and K. Lajtha. 1992. Plant spatial pattern and nutrient distribution in pinyon–juniper woodlands along an elevational gradient in northern New Mexico. *International Journal of Plant Science* **153**:425–433.
- Parsons, W. F. J., D. H. Knight, and S. L. Miller. 1994. Root gap dynamics in lodgepole pine forest: nitrogen transformations in gaps of different size. *Ecological Applications* **4**:354–362.
- Peitgen, H.-O., and D. Saupe. 1988. *The science of fractal images*. Springer-Verlag, New York, New York, USA.
- Peters, R. L., and J. D. Darling. 1985. The greenhouse effect and nature reserves. *BioScience* **35**:707–717.
- Pielke, R. A., and R. Avissar. 1990. Influence of landscape structure on local and regional climate. *Landscape Ecology* **4**:133–155.
- Rasure, J. R., and C. S. Williams. 1991. An integrated data flow visual language and software development environment. *Journal of Visual Languages and Computing* **2**:217–246.
- Reynolds, P. J., H. E. Stanley, and W. Klein. 1980. Large-cell Monte Carlo renormalization group for percolation. *Physical Review B* **21**:1223.
- Rich, P. M., G. S. Hughes, and F. J. Barnes. 1993. Using GIS to reconstruct canopy architecture and model ecological processes in pinyon–juniper woodlands. *Proceedings of the Thirteenth Annual Environmental Systems Research Institute (ESRI) User Conference*. Volume 2:435–445.
- Risser, P. G. 1995. The status of the science of examining ecotones. *BioScience* **45**:318–325.
- Rosen, R. 1989. Similitude, similarity, and scaling. *Landscape Ecology* **3**:207–216.
- Roux, S., and E. Guyon. 1991. Directed percolation front in a gradient. *Journal of Physics A* **24**:1611–1623.
- Scheuring, I., and R. H. Riedi. 1994. Application of multifractals to the analysis of vegetation pattern. *Journal of Vegetation Science* **5**:489–495.
- Sheaffer, J. D., and E. R. Reiter. 1985. Influence of Pacific sea surface temperatures on seasonal precipitation over the Western Plateau of the United States. *Archives for Meteorology, Geophysics, and Bioclimatology, Series A* **34**:111–130.
- Solé, R. V., and S. C. Manrubia. 1995. Are rainforests self-organized in a critical state? *Journal of Theoretical Biology* **173**:31–40.
- Stauffer, D. 1985. *Introduction to percolation theory*. Taylor and Francis, London, England.
- Stephenson, N. L. 1990. Climatic control of vegetation distribution: the role of water balance. *American Naturalist* **135**:649–670.
- Thom, R. 1975. *Structural stability and morphogenesis*. W. A. Benjamin, Reading, Massachusetts, USA.
- Tou, J. T., and R. C. Gonzalez. 1974. *Pattern recognition principles*. Addison-Wesley, Reading, Massachusetts, USA.
- Turner, M. G. 1989. Landscape ecology: the effect of pattern on process. *Annual Review of Ecology and Systematics* **20**:171–197.
- Van Devender, T. R., and W. G. Spaulding. 1979. Development of vegetation and climate in the southwestern United States. *Science* **204**:701–710.
- Voss, R. F. 1988. Fractals in nature: from characterization to simulation. Pages 21–70 in H.-O. Peitgen and D. Saupe, editors. *The science of fractal images*. Springer-Verlag, New York, New York, USA.

- West, N. 1984. Successional patterns and productivity potentials of pinyon–juniper ecosystems. Pages 1301–1332 in *Developing strategies for range management*. Westview, Boulder, Colorado, USA.
- West, N. E., K. H. Rhea, and R. J. Tausch. 1975. Basic synecological relationships in juniper–pinyon woodlands. Pages 41–53 in G. F. Gifford and F. E. Busby, editors. *The pinyon–juniper ecosystem: a symposium*. Utah Agricultural Experiment Station, Logan, Utah, USA.
- West, N. E., and N. S. Van Pelt. 1987. Successional patterns in pinyon–juniper woodlands. Pages 43–52 in R. L. Everett, editor. *Proceedings—pinyon–juniper conference*. U.S. Department of Agriculture Forest Service General Technical Report INT-215.
- Whittaker, R. H. 1967. Gradient analysis of vegetation. *Biological Reviews* 42:207–264.
- Wilcox, B. P. 1994. Runoff and erosion in intercanopy zones of pinyon–juniper woodlands. *Journal of Range Management* 47:285–295.
- Woodward, I. 1987. *Climate and plant distribution*. Cambridge University Press, New York, New York, USA.
- Yamamura, N. 1976. A mathematical approach to spatial distribution and temporal succession in plant communities. *Bulletin of Mathematical Biology* 38:517–526.
- Zallen, R. 1983. *The physics of amorphous solids*. John Wiley and Sons, New York, New York, USA.
- Zhu, Z., and D. L. Evans. 1994. U.S. forest types and predicted percent forest cover from AVHRR data. *Photogrammetric Engineering and Remote Sensing* LX(5):525–531.